Closed-form, localized wave solutions in optical fiber waveguides

Ashish M. Vengsarkar* and Ioannis M. Besieris

Bradley Department of Electrical Engineering, Virginia Polytechnic Institute and State University, Blacksburg, Virginia 24061-0111

Amr M. Shaarawi

Department of Engineering Physics and Mathematics, Faculty of Engineering, Cairo University, Giza, Egypt

Richard W. Ziolkowski

Electromagnetics Laboratory, ECE Building 104, Room 422E, University of Arizona, Tucson, Arizona 85721

Received June 6, 1991; accepted September 11, 1991; final revised manuscript received December 18, 1991

A novel bidirectional decomposition of exact solutions to the scalar wave equation has been shown to form a natural basis for synthesizing localized-wave (LW) solutions that describe localized, slowly decaying transmission of energy in free space. We present a theoretical feasibility study that shows the existence of LW solutions in optical fiber waveguides. As with the free-space case, these optical waveguide LW solutions propagate over long distances, undergoing only local variations. Four different source modulation spectra that give rise to solutions similar to focus wave modes, splash pulses, the scalar equivalent of Hillion's spinor modes, and the modified power spectrum pulses are considered. A detailed study of the modified power spectrum pulse is performed, the practical issues regarding the source spectra are addressed, and the distances over which such LW solutions maintain their nondecaying nature are quantified.

1. INTRODUCTION

Brittingham's pioneering work[1] in finding focus wave mode (FWM) solutions to Maxwell's equations has inspired several researchers to explore the existence of nondispersive, packetlike solutions to the wave equation that can propagate through free space without any decay. Ziolkowski[2] has argued that, although the FWM solutions have an infinite total energy content, a superposition of FWM's might have an advantage over the standard plane-wave superposition when it comes to describing the transfer of directed pulses in free space. Such pulses, characterized by high directionality and slow energy decay, have been termed localized waves (LW's).

Experimental investigations of launching acoustical LW's have shown considerable success. It has been established that a LW pulse launched from a linear synthetic array propagates with little variation over extended near-field distances. Recent results[3] have shown that a 10-fold improvement over continuous excitations is possible. Another area of research that is based on similar underlying principles is Durnin's diffraction-free Bessel beam.[4] Experimental verification of the larger depth of such a beam, as compared with a Gaussian beam, has been provided by Durnin *et al.*[5]

To assimilate all these attempts toward synthesizing highly directional pulses and beams into one representation, Besieris *et al.*[6] have proposed a novel approach to the synthesis of wave signals. Within the framework of this new approach, exact solutions are decomposed into bidirectional, backward and forward, plane waves traveling along a preferred direction z, viz., $\exp[-i\alpha(z - ct)]\exp[-i\beta(z + ct)]$. These bilinear expressions can be elementary solutions to the Fourier-transformed (with respect to x and y) three-dimensional wave equation, provided that a constraint relationship involving α, β, and the Fourier variables dual to x and y is satisfied. Such blocks have been shown to constitute a natural basis for synthesizing Brittinghamlike solutions, such as Ziolkowski's splash pulses, Hillion's spinor modes,[7] and the Ziolkowski–Belanger–Sezginer scalar FWM's. An application of this technique to infinitely long, cylindrical, metallic waveguides has been discussed by Shaarawi *et al.*[8] By varying the free parameters of specific source modulation spectra, one can synthesize within the waveguide the localized, nondecaying pulses that move predominantly in the positive direction. Questions about the physical nature and the causality of the bidirectional representation have been thoroughly addressed and will be presented elsewhere.[9]

In this paper we apply the method of bidirectional decomposition to optical fiber waveguides and investigate the possibility of synthesizing pulsed solutions that can propagate along such guides with only local variations. The analysis is similar to that of the infinite waveguide described by Shaarawi *et al.*,[8] with the exception of the boundary conditions that the fields must satisfy at the core–cladding interface. For simplicity, the core and the cladding materials are assumed to be both nondispersive and nonabsorptive. The only dispersive characteristics are due solely to the core–cladding interface. The general solution to the scalar wave equation in an optical fiber is analyzed for four source modulation spectra, and

0740-3232/92/060937-13$05.00

the approximations that need to be made to generate solutions similar to FWM's, splash pulses, the scalar equivalent of Hillion's spinor modes, and the modified power spectrum (MPS) pulses are considered.

Current research efforts in the area of high-speed, long-distance fiber-optic communications are concentrated on the development of new methods that will counter the pulse dispersion effects introduced during information transmission. The transmission of stationary, nonlinear optical pulses, termed solitons, in dispersive optical fibers was proposed by Hasegawa and Tappert[10] in 1973 and demonstrated in practice by Mollenauer *et al.*[11] in 1980. While soliton-based communications systems are on the verge of becoming a practical reality, limitations imposed on system performance by fiber loss, frequency chirp, and the interaction of neighboring pulses are still being studied. We propose a novel method of wave synthesis that does not invoke the need for nonlinear effects in optical fibers and that leads to solutions that are capable of countering the dispersive effects introduced by the waveguide. Although only an elementary theoretical discussion is presented in this paper, this technique may lead to the emergence of a competing technology in the area of high-capacity, fiber-optic communications.

In Section 2 we analyze the optical waveguide by assuming a solution of the bidirectional type and arrive at a generic elementary solution to the scalar equation in terms of the newly defined parameters. In Section 3 we take recourse to the classical waveguide analysis to simplify the generic solution further. A one-to-one correspondence is established between the two methods, and the conditions for the core and the cladding regions are established. This leads to an elimination of the practically unrealizable solutions and simplifies the mathematical analysis that follows. In Section 4 we briefly describe the linearly polarized (LP) modes in the optical fiber and use the properties derived in the literature to specify the boundary conditions. The superposition of the elementary solutions obtained after the boundary conditions have been invoked is described in Section 5. In Section 6 we consider the singular source spectrum, the splash pulse spectrum, the zero-order Bessel spectrum, and the MPS spectrum and derive expressions for pulselike solutions in optical fibers. In Section 7 we evaluate the nondecaying nature of the MPS pulse shape and relate the free parameters to physically meaningful quantities. We quantify the distance for which no decay will be observed in the MPS pulse solution derived earlier. The feasibility of practical implementation of such spectra as well as future theoretical directions are considered in the concluding section.

2. SCALAR WAVE EQUATION

The scalar wave equation for an idealized optical fiber made of a nondispersive and nonabsorptive material can be written as

$$\left(\nabla^2 - \frac{n_i^2}{c^2}\partial_t^2\right)\Psi_i = 0, \qquad i = 1 \Rightarrow \text{core}, \quad i = 2 \Rightarrow \text{cladding}, \tag{1}$$

where ∇^2 is the three-dimensional Laplacian, n is the refractive index ($n_1 > n_2$; n_1, n_2 assumed to be constant), and c is the velocity of light *in vacuo*.

According to the bidirectional decomposition,[6] we assume a solution of the type

$$\Psi(\rho,\phi,z,t) = \Phi(\rho,\phi)\exp[i\beta(z+ct)]\exp[-i\alpha(z-ct)] = \Phi(\rho,\phi)\exp(i\beta\eta)\exp(-i\alpha\zeta), \tag{2}$$

where $\eta = z + ct$ and $\zeta = z - ct$. Breaking up the Laplacian into its transverse component ∇_t^2 and a longitudinal component ∂_z^2, we can write the following:

$$\partial_z^2\Psi = -(\beta-\alpha)^2\Psi, \tag{3}$$

$$\partial_t^2\Psi = -c^2(\beta+\alpha)^2\Psi. \tag{4}$$

Equation (1) then becomes

$$(\nabla_t^2 + \kappa_i^2)\Phi = 0, \tag{5}$$

where $\kappa_i^2 = n_i^2(\alpha+\beta)^2 - (\alpha-\beta)^2$. In cylindrical coordinates, ∇_t^2 is given by

$$\nabla_t^2 = \partial^2/\partial\rho^2 + \rho^{-1}\partial/\partial\rho + \rho^{-2}\partial^2/\partial\phi^2. \tag{6}$$

Substituting Eq. (6) into Eq. (5) and assuming separability with respect to the variables ρ and ϕ, viz., $\Phi(\rho,\phi) = R(\rho)F(\phi)$, we get a set of ordinary differential equations; specifically,

$$\mathrm{d}^2R/\mathrm{d}\rho^2 + \rho^{-1}\mathrm{d}R/\mathrm{d}\rho + (\kappa_i^2 - \nu^2/\rho^2)R = 0, \tag{7}$$

$$\mathrm{d}^2F/\mathrm{d}\phi^2 + \nu^2F = 0. \tag{8}$$

Equation (7) is the Bessel differential equation, and Eq. (8) is the second-order, ordinary, harmonic differential equation. Solving Eqs. (7) and (8) and recombining variables, we can write a general solution to the Helmholtz equation [Eq. (5)] as

$$\Phi(\rho,\phi) = \begin{cases} AJ_\nu(\kappa_i\rho) + BY_\nu(\kappa_i\rho) \\ CI_\nu(\kappa_i\rho) + DK_\nu(\kappa_i\rho) \end{cases}\cos\nu\phi, \qquad \begin{matrix}\kappa_i^2 > 0 \\ \kappa_i^2 < 0\end{matrix}, \tag{9}$$

where A, B, C, and D are constants and J_ν, Y_ν, I_ν, and K_ν are the ordinary and the modified Bessel functions. In the classical analysis of a waveguide solution, one would determine which of these constants need to be zero so as to acquire practically realizable solutions. To do that, we first determine the respective regions of the waveguide in which $\kappa_i^2 > 0$ and $\kappa_i^2 < 0$.

3. CLASSICAL WAVEGUIDE ANALYSIS

We seek to establish a one-to-one correspondence between the parameters in the bidirectional approach and the classical analysis. Since the waveguiding conditions that the mode propagation constant β_{cl} should satisfy are known in a classical analysis, the one-to-one correspondence will determine the constraints on the parameters α and β as well as help in establishing the regions denoted by $\kappa_i^2 > 0$ and $\kappa_i^2 < 0$. This is a valid means of obtaining some of the desired conditions because the bidirectional decomposition is an alternative method for the synthesis of pulselike solutions and not a replacement for the classical Fourier synthesis. There exists a parallel between the two methods, and it is most advantageous to extract maximum information from each of these approaches.

In the classical analysis we consider solutions of the form

$$\Psi(\rho,\phi,z,t) = \Phi(\rho,\phi)\exp(\pm i\beta_{cl}z)\exp(+i\omega_{cl}t), \tag{10}$$

where β is the propagation constant, ω is the angular frequency given by $2\pi c/\lambda$ in terms of the wavelength, and the subscript cl is used to denote the classical approach. Comparing Eqs. (10) and (2), we can show the correspondence

$$\beta_{cl} \leftrightarrow (\beta - \alpha), \qquad \omega_{cl} \leftrightarrow -(\alpha + \beta)c \tag{11a}$$

or

$$\beta_{cl} \leftrightarrow (\alpha - \beta), \qquad \omega_{cl} \leftrightarrow (\alpha + \beta)c. \tag{11b}$$

The classical waveguiding condition in this case is given by

$$n_2\omega_{cl} < \beta_{cl}c < n_1\omega_{cl}, \tag{12}$$

which can also be expressed as the set of expressions

$$(n_1\omega_{cl})^2 - (\beta_{cl}c)^2 > 0, \tag{13a}$$

$$(\beta_{cl}c)^2 - (n_2\omega_{cl})^2 > 0. \tag{13b}$$

The corresponding expressions for the bidirectional approach give us

$$n_1{}^2(\alpha + \beta)^2 - (\alpha - \beta)^2 > 0, \tag{14a}$$

$$n_2{}^2(\alpha + \beta)^2 - (\alpha - \beta)^2 < 0, \tag{14b}$$

thereby implying that $\kappa_1{}^2 > 0$ and $\kappa_2{}^2 < 0$. Elementary solutions for the Helmholtz equation [Eq. (5)] in the two regions of interest, the core and the cladding, are given by Eq. (9). Since $Y_\nu(\kappa_1\rho) \to \infty$ for $\rho = 0$ and $I_\nu(\kappa_2\rho) \to \infty$ as $\rho \to \infty$, the constants B and C are taken to be zero so that physically realizable solutions are obtained. Further, for simplicity of analysis we assume that there is no azimuthal dependence of the field ($\nu = 0$). Hence the solution simplifies to

$$\Phi(\rho) = \begin{cases} AJ_0(\kappa_1\rho), & \rho < a \\ DK_0(\kappa_2\rho), & \rho > a \end{cases}. \tag{15}$$

The constants A and D are determined in Section 4.

4. LINEARLY POLARIZED MODES IN WEAKLY GUIDING FIBERS

In most practical optical fibers, the refractive indices of the core and of the cladding are nearly equal. If the parameter Δ is defined as

$$\Delta = \frac{n_1{}^2 - n_2{}^2}{2n_1{}^2} \cong \frac{n_1 - n_2}{n_1}, \tag{16}$$

then the condition $\Delta \ll 1$ is called the weak-guidance condition, and an optical fiber with this property is called a weakly guiding fiber. With this weak-guidance condition, we can simplify the exact solutions of Maxwell's equations to give an insight into the properties of certain combinations of modes, termed LP modes. Apart from the simplification in the analysis and the ease in understanding the mode phenomena, the concept of LP modes has other useful properties. Gloge[12] has shown that it is possible to calculate the fields in the fiber and the characteristic equations of LP modes directly from Maxwell's equations. The solutions so obtained are based on the scalar wave equation, and for this reason the LP modes are sometimes referred to as scalar modes.

These properties of LP modes imply that the solution $\Phi(\rho, \phi)$ in Eq. (15) can be considered a representation of the LP_{01} mode of a fiber, the first subscript denoting that $\nu = 0$. To find a relation between the constants A and D in Eq. (15), we use the property of LP modes that, to meet all boundary conditions, it is sufficient that Φ and $d\Phi/d\rho$ be continuous at $\rho = a$, where a is the radius of the fiber.[12] This leads us to our final expression for the elementary solution for the Helmholtz equation [Eq. (5)], viz.,

$$\Phi(\rho) = \begin{cases} AJ_0(\kappa_1\rho), & \rho < a, \\ \dfrac{AK_0(\kappa_2\rho)}{K_0(\kappa_2 a)}J_0(\kappa_1 a), & \rho > a \end{cases} \tag{17}$$

as well as to the characteristic equation of the fiber

$$\frac{\kappa_1 J_1(\kappa_1 a)}{J_0(\kappa_1 a)} = \frac{\kappa_2 K_1(\kappa_2 a)}{K_0(\kappa_2 a)}, \tag{18}$$

where we have used the property of the Bessel functions, $J_0'(\kappa_1 a) = -J_1(\kappa_1 a)$ and $K_0'(\kappa_2 a) = -K_1(\kappa_2 a)$, where the primes indicate derivatives with respect to the arguments of the Bessel functions.

5. GENERALIZED SOLUTION

We now develop the generalized solution to the scalar wave equation by using the bidirectional representation. In the analysis that follows, the constraint on α and β, given by the equation $\kappa_i{}^2 = n_i{}^2(\alpha + \beta)^2 - (\alpha - \beta)^2$, is difficult to handle. For this reason, we model the waveguide as one with a core of refractive index $n_1 = 1$ and a cladding of effective refractive index $n_2 = n_e (n_e < 1)$. It is fairly simple to calculate this effective index n_e, as shown in Appendix A. This change in notation for the refractive indices alters the constraints to

$$\kappa_1{}^2 = 4\alpha\beta, \tag{19a}$$

$$\kappa_2{}^2 = n_e{}^2(\alpha + \beta)^2 - (\alpha - \beta)^2. \tag{19b}$$

A general solution to the scalar wave equation can be written in terms of the superposition

$$\Psi(\rho, \zeta, \eta) = \frac{1}{(2\pi)^2}\int d\kappa_1 \int d\alpha \int d\beta A(\alpha, \beta, \kappa_1)\kappa_1 J_0(\kappa_1\rho) \times \exp(-i\alpha\zeta)\exp(i\beta\eta)\delta(4\alpha\beta - \kappa_1{}^2) \tag{20}$$

for $\rho \le a$, where the constraint of Eq. (19a) has been incorporated within the integral with the help of the delta function. Similarly, for the region $\rho \ge a$ we have

$$\Psi(\rho, \zeta, \eta) = \frac{1}{(2\pi)^2}\int d\kappa_1 \int d\kappa_2 \int d\alpha \int d\beta A(\alpha, \beta, \kappa_1)\kappa_1 K_0(\kappa_2\rho) \times \frac{J_0(\kappa_1 a)}{K_0(\kappa_2 a)}\exp(-i\alpha\zeta)\exp(i\beta\eta)\delta[\kappa_2 - f(\kappa_1)] \times \delta(4\alpha\beta - \kappa_1{}^2)\delta[\kappa_2{}^2 - n_e{}^2(\alpha + \beta)^2 + (\alpha - \beta)^2], \tag{21}$$

which includes all the boundary conditions that Φ should satisfy at $\rho = a$ as well as the constraints of Eqs. (18) and (19). In Eq. (21) $f(\kappa_1)$ denotes the constraint imposed on the choice of κ_2 once a value is chosen for κ_1 and can be evaluated from the characteristic equation (18). A numerical evaluation of Eq. (18) gives the functional relationship between κ_2 and κ_1 and is shown in Fig. 1.

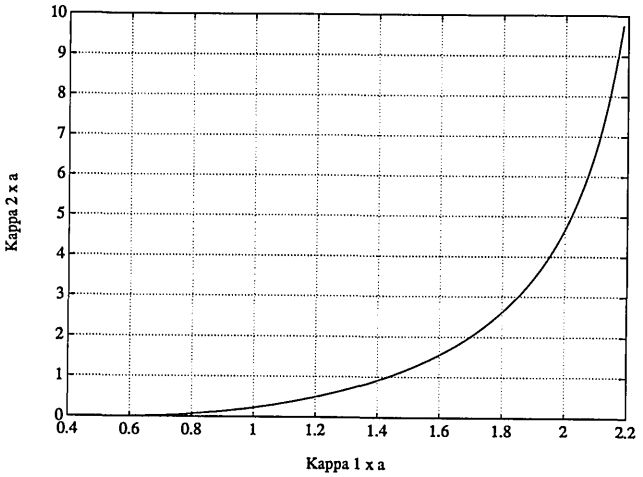

Fig. 1. Dependence of the cladding parameter κ_2 on the choice of values for the core parameter κ_1. The graph defines the function $f(\kappa_1)$ in the text.

The limits on the integrals in Eqs. (20) and (21) will be dependent on the constraints given by expression (12) along with the two choices for the one-to-one correspondence between the classical analysis and the bidirectional approach, expressions (11a) and (11b):

Choice 1: Expressions (11a) reduce constraint expression (12) to

$$-n_2(\alpha + \beta) < (\beta - \alpha) < -n_1(\alpha + \beta), \tag{22}$$

which, for $n_1 = 1$ and $n_2 = n_e$, gives us the two conditions

$$\alpha/\beta < s, \qquad \alpha\beta < 0, \tag{23}$$

where $s = [(1 + n_e)/(1 - n_e)]$. As a consequence, the limits of the integrals in Eq. (20) and (21) can be written as

$$\int_0^\infty d\kappa_i \int_{-\infty}^0 d\beta \int_0^{\beta s} d\alpha I \tag{24}$$

or

$$\int_0^\infty d\kappa_i \int_{-\infty}^0 d\alpha \int_0^{\alpha/s} d\beta I, \tag{25}$$

where I represents the integrand in each of the integrals. The order in which the integrations are carried out (first over the variable α and then over β or vice versa) determines which of the above two expressions is applicable. In expression (24) we note, however, that, since β is always negative, the integration over α is from zero to a negative number, βs ($s > 0$). But α should always be positive to satisfy the condition $\alpha\beta < 0$. Hence expression (24) gives us a contradiction in terms and leads to a trivial solution that is always equal to zero. This is a mathematical verification of the fact that the boundary conditions do not match. Similarly, we can show that changing the order of integration [cf. expression (25)] will also lead to a situation in which both conditions (23) cannot be satisfied.

Choice 2: Expressions (11b) reduce constraint expression (12) to

$$n_2(\alpha + \beta) < (\alpha - \beta) < n_1(\alpha + \beta), \tag{26}$$

which, for $n_1 = 1$ and $n_2 = n_e$, gives us the two conditions

$$\alpha/\beta > s, \qquad \alpha\beta > 0. \tag{27}$$

As a result, the limits of the integrals in Eqs. (20) and (21) can be written, for the case when both α and β are greater than zero, as

$$\int_0^\infty d\kappa_i \int_0^\infty d\beta \int_{\beta s}^\infty d\alpha I \tag{28}$$

or

$$\int_0^\infty d\kappa_i \int_0^\infty d\alpha \int_0^{\alpha/s} d\beta I, \tag{29}$$

where I represents the integrand in each of the integrals. With this choice of the one-to-one correspondence, it is possible to satisfy both conditions (27). Also, in the limit $n_e \to 1$, we would expect that the solution should vanish since the waveguiding constraint is no longer met. This is evident from the limits, since $s \to \infty$, and integrals (28) and (29) go to zero for any integrand.

The generalized solutions [Eqs. (20) and (21)] were obtained under the assumption that the constraints [expression (26)] are satisfied in all the regions. Hence the limits in integrals (28) and (29) are applicable to the evaluation of the generalized solutions in the core as well as the cladding region.

6. PULSELIKE SOLUTIONS IN OPTICAL FIBERS

Different choices of the modulation spectrum $A(\alpha, \beta, \kappa)$ entering into the bidirectional representations [Eqs. (20) and (21)] can now lead to the desired packetlike solutions. In this section we consider four specific spectra and derive solutions that resemble the ideal FWM, the scalar analog to Hillion's spinor modes, the ideal splash pulse, and the ideal MPS pulse. It is interesting to note in the analysis that follows that the simplicity of the final expressions for the localized solutions depends on the order in which the integrations in Eq. (21) are carried out. For instance, the integration, first over α and then over β, described by expression (28) would likely lead to a compact solution in the form of an integral that may need numerical evaluation. On the other hand, if the order of integration is reversed, as described by expression (29), we may be able to extract information about the ideal free-space solution that the pulse would resemble. In such cases the solution Ψ is broken into two parts, viz., $\Psi = \Psi_u + \Psi_w$, where the subscript u indicates the unperturbed packetlike solution and the subscript w stands for the additional wall term introduced by the waveguiding constraint.

In the following subsections we summarize the results obtained from the synthesis of four different spectra; the details of the derivations are provided in Appendix B. A discussion of the physical implications is given in Section 7.

A. Focus Wave Modes

We first consider the singular spectrum

$$A(\alpha, \beta, \kappa_1) = (8\pi^2 a_1)\delta(\beta - \beta')\exp(-\alpha a_1), \tag{30}$$

which, in free space, has given rise to FWM's, as introduced by Belanger,[13] Sezginer,[14] and Ziolkowski.[15] The constants a_1 and β' are free parameters in the source modulation spectrum that will be useful in adjusting the synthesized solutions to give directed energy transfer in the waveguide.

Substituting the singular spectrum [Eq. (30)] into the bidirectional representation [Eq. (20)] and carrying out the details shown in Appendix B, we get the expression for the ideal FWM solution [see Eq. (B6)]:

$$\Psi_u = \frac{a_1 \exp(i\beta'\eta)}{(a_1 + i\zeta)} \exp\left[-\frac{\beta'\rho^2}{(a_1 + i\zeta)}\right], \tag{31}$$

which is identical to that given by Ziolkowski.[15] The wall term is found to be, from Eq. (B10),

$$\begin{aligned}\Psi_w = {} & \frac{ia_1}{(a_1 + i\zeta)} \exp[\beta'(a_1 + i\zeta)s] \\ & \times \{U_1[-2i\beta'(a_1 + i\zeta)s, 2\rho\beta'\sqrt{s}\,] \\ & + iU_2[-2i\beta'(a_1 + i\zeta)s, 2\rho\beta'\sqrt{s}\,]\},\end{aligned} \tag{32}$$

where $s = [(1 + n_e)/(1 - n_e)]$ and U is the Lommel function of two variables defined in Appendix B.

A similar analysis can now be extended to the scalar field solution in the cladding. The constraints imposed by the delta functions in Eq. (21), however, necessitate the use of a numerical integration, and we do not address that issue in this paper.

B. Splash Pulses

We consider next the spectrum

$$A_0(\alpha, \beta, \kappa_1) = 8\pi^2 a_1 a_2 \delta(\kappa_1 - \gamma)\exp[-(\alpha a_1 + \beta a_2)], \tag{33}$$

which, without the delta function, yields Ziolkowski's splash pulse in free space.[2] Equations (B13) and (B14) from Appendix B give us

$$\Psi_u = a_1 a_2 \gamma J_0(\gamma\rho) K_0\{\gamma[(a_1 + i\zeta)(a_2 - i\eta)]^{1/2}\}, \tag{34}$$

$$\begin{aligned}\Psi_w = {} & -\frac{a_1 a_2 \gamma}{2} \int_0^{\gamma\sqrt{s}/2} \frac{d\alpha}{\alpha} \exp[-\alpha(a_1 + i\zeta)] \\ & \times \exp\left[\frac{\gamma^2}{4\alpha}(a_2 - i\eta)\right]\end{aligned} \tag{35}$$

in the fiber core. The expressions for the cladding region can be obtained by numerical methods, similar to the case of the FWM solutions in Section 5.

C. Scalar Analog to Hillion's Spinor Modes

We consider next the Bessel spectrum of order zero,

$$A_0(\alpha, \beta, \kappa_1) = 8\pi^2 a_1 b J_0(\beta b)\exp(-\alpha a_1), \tag{36}$$

which, in free space, yields the scalar analog to Hillion's spinor modes.[7] Integrating first over β and then over α, we find the total solution to be, from Eq. (B19) of Appendix B,

$$\begin{aligned}\Psi = {} & a_1 b \int_0^{\theta_1} d\theta \frac{p}{(qd)^{1/2}[(\rho^2 + q^2 + d^2) - 4q^2 d^2]^{1/2}} \\ & \times Q_{-1/2}{}^1\left(\frac{p^2 + q^2 + d^2}{2qd}\right),\end{aligned} \tag{37}$$

where $\tan\theta_1 = s$, $p = (a_1 + i\zeta)\cos\theta - i\eta\sin\theta$, $q = 2\rho(\sin\theta\cos\theta)^{1/2}$, $d = b\sin\theta$, and $Q_n{}^m(z)$ is an associated Legendre function described in Appendix B. To obtain a physical understanding of the pulse behavior described by Eq. (38), we reverse the order of integration and obtain the expressions for Ψ_u and Ψ_w, given by Eqs. (B24) and (B26):

$$\Psi_u = \frac{a_1 b}{(a_1 + i\zeta)} \left\{\left[\frac{\rho^2}{(a_1 + i\zeta)} - i\eta\right]^2 + b^2\right\}^{-1/2}, \tag{38}$$

$$\begin{aligned}\Psi_w = {} & \frac{ia_1 b}{(a_1 + i\zeta)} \int_0^\infty d\beta \exp\{-\beta[(a_1 + i\zeta)s - i\eta]\} \\ & \times \{U_1[-2i\beta(a_1 + i\zeta)s, 2\rho\beta\sqrt{s}\,] \\ & + iU_2[-2i\beta(a_1 + i\zeta)s, 2\rho\beta\sqrt{s}\,]\}.\end{aligned} \tag{39}$$

D. Modified Power Spectrum Pulse

We now consider the MPS pulse spectrum

$$A(\alpha, \beta, \kappa) = \begin{cases} \frac{\pi p}{2} \exp[-\alpha a_1 - (p\beta - b)a_2], & \beta > b/p \\ 0, & b/p > \beta > 0 \end{cases}, \tag{40}$$

which leads to localized, slowly decaying solutions in free space.[6] Substituting the spectrum from Eq. (40) into expression (28), we arrive at the expressions for Ψ_u and Ψ_w of the MPS pulse given by Eq. (B29) and expression (B32) in Appendix B:

$$\Psi_u(\rho, \zeta, \eta) = \frac{\exp[-(b\chi/p)]}{4\pi(a_1 + i\zeta)(a_2 + \chi/p)}, \tag{41}$$

$$\begin{aligned}\Psi_w \approx {} & \frac{ip\exp(ba_2)}{2\pi(a_1 + i\zeta)} \exp\left(-\frac{b}{p}\Omega\right) \\ & \times \left\{U_1\left[2i\frac{b}{p}(a_1 + i\xi)s, 2\rho\frac{b}{p}\sqrt{s}\,\right]\right. \\ & \left. + iU_2\left[2i\frac{b}{p}(a_1 + i\xi)s, 2\rho\frac{b}{p}\sqrt{s}\,\right]\right\},\end{aligned} \tag{42}$$

where

$$\chi = \frac{\rho^2}{a_1 + i\zeta} - i\eta, \tag{43}$$

$$\Omega = (pa_2 - i\eta) + s(a_1 + i\zeta). \tag{44}$$

7. DETAILED STUDY OF THE MODIFIED POWER SPECTRUM PULSE

Equations (31), (34), (38), and (41) for Ψ_u represent the nondecaying, ideal, LW solutions in the core for the FWM's, the splash pulses, the scalar equivalent of Hillion's spinor modes, and the MPS pulses, respectively, while Eqs. (32), (35), and (39) and relation (42) for Ψ_w describe the deviations in those free-space solutions that are due to the waveguiding constraint. The behavior of these solutions is sensitive to the values of the free parameters a_1, a_2, b, p, γ, and β'. To understand the properties of these solutions, we analyze the pulses as they propagate through the waveguide and quantify the distances over which they maintain their nondecaying nature. Substituting values

of the free parameters in the source modulation spectra into the equations, we will be able to determine the amount of localization of the initial pulse and the behavior of the pulses traveling in the positive and the negative directions. By doing so, we will relate the free parameters in the spectra to physically meaningful quantities, such as the width of the initial pulse and its amplitude.

We note that Eqs. (32), (35), (39), and (40) for Ψ_w can be evaluated numerically only for specific values of the free parameters. In this section we restrict ourselves to a detailed analysis and quantification of the MPS pulse for which a tractable, closed-form solution is available. However, to gain a better understanding of the properties of the ideal pulses resulting from the remaining spectra, we have determined the nature of the free parameters in the spectra and their effect on the unperturbed, ideal pulse shapes and amplitudes. A description is given in Appendix C.

A. Similarity to Free-Space Modified Power Spectrum Pulse

It is known that the unperturbed MPS pulse is localized in space and can propagate without decay for thousands of kilometers (for an appropriate choice of the free parameters). We therefore compare the relative amplitudes of the unperturbed and the wall terms for a specific case, namely, at $\rho = 0$ and $z = 0$. We use the Bessel-function expansion of Lommel functions [See Eq. (B9) of Appendix B] to evaluate the wall term at $\rho = 0$. Using l'Hôpital's rule and the recursive relations for Bessel functions, we can show that

$$\lim_{z\to 0} \frac{J_m(\alpha z)}{z^m} = \frac{\alpha^m}{m!2^m}. \tag{45}$$

The wall term Ψ_w can be expressed at $\rho = 0$ and $z = 0$, from expression (42) and Eq. (45), as

$$|\Psi_w(\rho = 0, z = 0)| = \frac{1}{2\pi a_1 a_2}\left[1 - \exp\left(-\frac{a_1 s b}{p}\right)\right], \tag{46}$$

where we have assumed that $pa_2 \gg sa_1$. The ratio of the unperturbed term to the wall term then becomes

$$\frac{|\Psi_u|}{|\Psi_w|} = \frac{1}{2[1 - \exp(-x)]}, \tag{47}$$

where $x = sba_1/p$. For small values of x, this ratio becomes

$$\frac{|\Psi_u|}{|\Psi_w|} \approx \frac{1}{2x}, \tag{48}$$

which implies that, for a more pronounced localization of the total solution, one should choose the factor x to be small.

B. Practical Implications of Free Parameters

Using our knowledge from the analysis of the free-space MPS pulse,[6] we can now connect the behavior of the guided LW solution directly to the values of its defining constants. We intentionally fix the constant $a_2 = 1.0$ m; the other constants control the following properties.

Normalizing the magnitude of the solution Ψ at $\rho = 0$, $z = ct$, to its initial value $4\pi a_1 a_2$, we obtain

$$|\Psi(\rho = 0, z = ct)| = \frac{3}{[1 + (2z/pa_2)^2]^{1/2}}. \tag{49}$$

This means that the amplitude of the solution is maintained to the distance $L \approx pa_2$. Since we desire to maintain the initial amplitude over distances $L \sim 40{,}000$ km, we take p to be very large, i.e., $p = 10^8$.

Note that the choice of values for p is not completely determined by the localization distance L. The waist of the beam, as well as the minimum angular frequency $\omega_{\min}$, controls the value of p as shown below. The maximum angular frequency of interest, $\omega_{\max}$, is fixed by a_1 to be

$$\omega_{\max} = c/a_1, \tag{50}$$

and the minimum angular frequency $\omega_{\min}$ is fixed by the ratio b/p to be

$$\omega_{\min} = cb/p. \tag{51}$$

The transverse localization of the unperturbed MPS pulse is given by its initial waist,

$$w_0^2 = \frac{pa_1}{b} = \frac{\lambda_{\min}}{2\pi}\frac{\lambda_{\max}}{2\pi}, \tag{52}$$

where $\lambda_{\max} = 2\pi c/\omega_{\min}$ and $\lambda_{\min} = 2\pi c/\omega_{\max}$. Hence the waist is fixed if the minimum and the maximum wavelengths are specified. On the other hand,

$$\frac{b}{p} = \frac{a_1}{w_0^2} = \frac{2\pi}{\lambda_{\max}}. \tag{53}$$

Equations (52) and (53) imply that the maximum and the minimum wavelengths $\lambda_{\min}$ and $\lambda_{\max}$ are fixed if a_1 and w_0 are specified. Since in practice the available frequencies in the fiber are limited, we have chosen, for the sake of demonstration, $\lambda_{\min} = 0.3$ μm and $\lambda_{\max} = 30$ μm. The fiber dimensions limit the allowed choices for the waists. Since our wavelength selection gives $w_0 = 0.50$ μm, the initial waist is smaller than the chosen fiber radius ($r \approx 2$–5 μm). Then the ratio $b/p = 2.1 \times 10^5$ finally fixes the remaining constant b to be very large: $b = 2.1 \times 10^{13}$. Therefore the assumption that $a_1 \ll p/a_2$ or, since

$$x = \frac{sba_1}{p} = s\left(\frac{a_1}{w_0}\right)^2 \ll 1, \tag{54}$$

that $x \ll b/a_2$, which was used to obtain Eq. (49), is valid. In this small-x limit, expression (48) reduces to the form

$$\frac{|\Psi_u|}{|\Psi_w|} \approx \frac{1}{2x} = \frac{1}{2s}\frac{w_0^2}{a_1^2} = \frac{1}{2s}\frac{\lambda_{\max}}{\lambda_{\min}} = \frac{1}{2s}\frac{\omega_{\max}}{\omega_{\min}}. \tag{55}$$

This result indicates that an increase in the bandwidth or, equivalently, an increase in the number of minimum wavelengths in the waist will increase the difference between the unperturbed MPS core term and the wall term,

thus making the guided LW solution more like its free-space counterpart. The requirement that $x \ll 1$ sets a practical limitation on the fiber structure: Either the fiber material should be highly transparent to a broad window of wavelengths or the fiber should be strongly guiding. One would therefore have to explore materials with large transparent windows of transmission or reevaluate the entire analysis without using the LP mode formulation. The latter approach would necessitate the use of smaller-core fibers to remain close to single-mode operation and would in turn imply added complexity of source design. Equation (55) also underscores the contribution of the wall term as a function of the weak-guidance condition of the fiber. For example, if the index of refraction of the fiber cladding were made closer to the core refractive index, the fiber would guide the modes in a weaker fashion, and we would expect the contribution from the wall term to increase. This physical insight is confirmed by Eq. (55) since, as $n_e \to 1$, s increases and the ratio $|\Psi_u|/|\Psi_w|$ decreases, implying a growing influence of the wall term.

Returning to the explicit representation of the wall term [Eq. (43)], one finds that its transverse variations are controlled by the Lommel-function terms. Since

$$\sqrt{s}\frac{b}{p}\rho = 4\pi x\frac{\sqrt{s}}{\lambda_{\min}} \tag{56}$$

except when $\rho < \lambda_{\min}$, an explicit numerical evaluation of those terms is necessary. These terms yield an oscillatory, rapidly damped function of ρ. The decay rate can be obtained since, as $z \to \infty$, the function

$$\frac{J_n(\alpha z)}{z^n} \to (\alpha z^{2n+1})^{-1/2}, \tag{57}$$

so that only the $n = 1$ term survives, and it goes to zero like $(\rho/\lambda_{\min})^{-3/2}$. In contrast, the perturbed core term decays transversely as $\exp[-(\rho^2/w_0^2)]$ except in the (forward and backward) tail regions of the MPS pulse, where $|z - ct| \gg a_1$, so that the term's decay is more gradual,

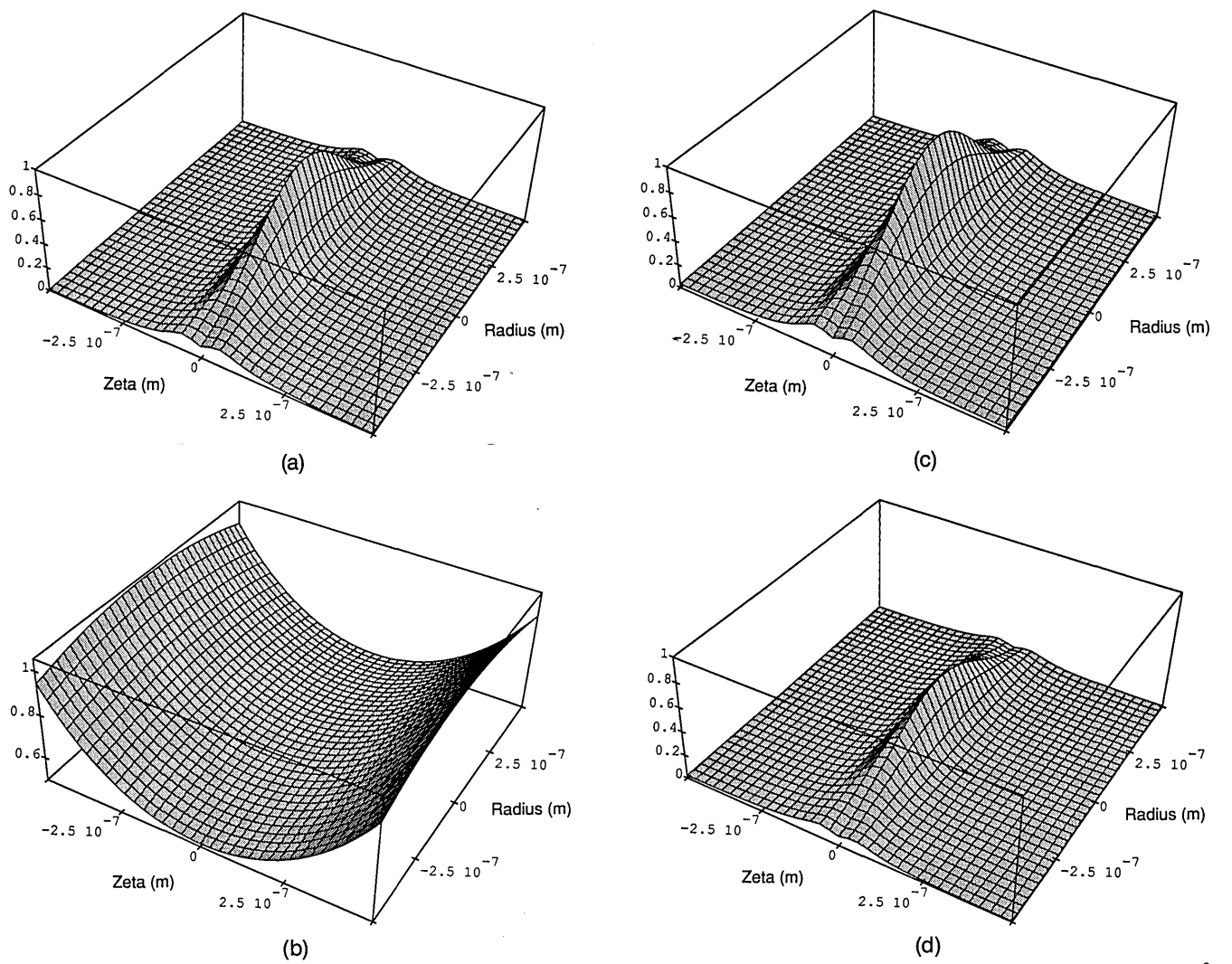

Fig. 2. Evolution of the MPS pulse as it propagates through the fiber. (a) $z = 0$. Normalized unperturbed free-space equivalent, $|\Psi_u|^2$. (b) $z = 0$ m. Normalized wall term, $|\Psi_w|^2$. (c) $z = 0$ m. Normalized total solution, $|\Psi_u + \Psi_w|^2$. (d) $z = 40{,}000$ km. The plots show that the MPS pulse remains localized over distances of the order of several thousand kilometers, starts decaying slowly when $z = 10{,}000$ km, and spreads out significantly (with a drop in peak amplitude) after propagating over a distance of 40,000 km. The parametric values used are $a_1 = 5 \times 10^{-8}$ m, $a_2 = 1$ m, $b = 2.1 \times 10^{13}$ m^{-1}, $p = 10^8$, and $s = 10$. These values correspond to $\lambda_{\max}/\lambda_{\min} = 100$.

similar to its axial decay:

$$\frac{\exp(-\{\rho^2/w_0{}^2[1+(z-ct)^2/a_1{}^2]\})}{1+(z-ct)^2/a_1{}^2} \sim \frac{\exp\{[\rho^2 a_1{}^2/w_0{}^2(z-ct)^2]\}}{1+(z-ct)^2/a_1{}^2} \sim \left[1+\frac{(z-ct)^2}{a_1{}^2}\right]^{-1}. \quad (58)$$

Thus, if the waist is many wavelengths in size, the wall term will be much smaller than the core term everywhere except near the wall, where its decay rate becomes slightly smaller than the core's. This comparison illustrates that the wall term in the forward tail region of the core MPS component will lead the central peak. This means that one can visualize the wall component of the guided LW solution as a low-level background field propagating in the fiber with little significant contribution except near the wall, where it provides a guiding and renovating mechanism for the central, core component. Heuristically, it appears that the core component surfs along in the fiber on the background wall field.

C. Graphic Description of Modified Power Spectrum

The variation of the square of the amplitude of the unperturbed solution, $|\Psi_u|^2$, for $\lambda_{max}/\lambda_{min} = 100$ is shown in Fig. 2(a). The corresponding wall term is shown in Fig. 2(b). Figure 2(c) shows the total launched pulse at the input end of the fiber ($z = 0$); for a fiber core diameter of the order of a few micrometers, the pulse is largely confined to the core. The total pulse looks exactly like the unperturbed solution, indicating that the effect of the wall term is negligible for this choice of free parameters. Local variations in the pulse shape are seen as a function of the parameter ζ. At distances of propagation of the order of several thousand kilometers, there is no variation in the amplitude of the pulse. At $z = 40{,}000$ km [shown in Fig. 2(d)], the localized nature of the solution starts collapsing, the pulse shape changes, and the peak amplitude drops to less than half the original amplitude. The plots in Fig. 2 were obtained for an x value of 0.2, and hence the contribution that is due to the wall term is not noticeable for a ratio $|\Psi_u|/|\Psi_w| = 5.0$. To emphasize the heuristic surfing nature of the unperturbed core term along the wall term, we plot the different components of the MPS pulse for $\lambda_{max}/\lambda_{min} = 25$ or, equivalently, for $|\Psi_u|/|\Psi_w| = 1.25$. These plots are shown in Fig. 3. Once again, the normalized unperturbed and wall terms behave like their counterparts in Fig. 2; however, the total pulse now appears to possess a noticeable contribution from the wall term. Note that in Figs. 2 and 3 the squares of the amplitudes are normalized; as a result, the total pulse solution should not be considered to be a mere sum of the individual contributions from the Ψ_u and the Ψ_w terms.

To ensure propagation of electromagnetic energy in the positive direction, it is instructional to analyze the behavior of the pulse traveling in the negative direction. We evaluated the behavior of the MPS pulse in the negative direction and found that the solution in the negative direction decays rapidly over distances of the order of 10^{-18} m and is of the order of 10^{-19} times the original pulse amplitude after propagating a distance of 1 m. This result further confirms that the choice of the free parameter values can lead to positive pulse propagation without any negative component's being supported by the waveguide.

Let us consider another example, in particular, the splash pulse spectrum. As we show in Appendix C, Subsection 4, for longitudinal amplitude maintenance along

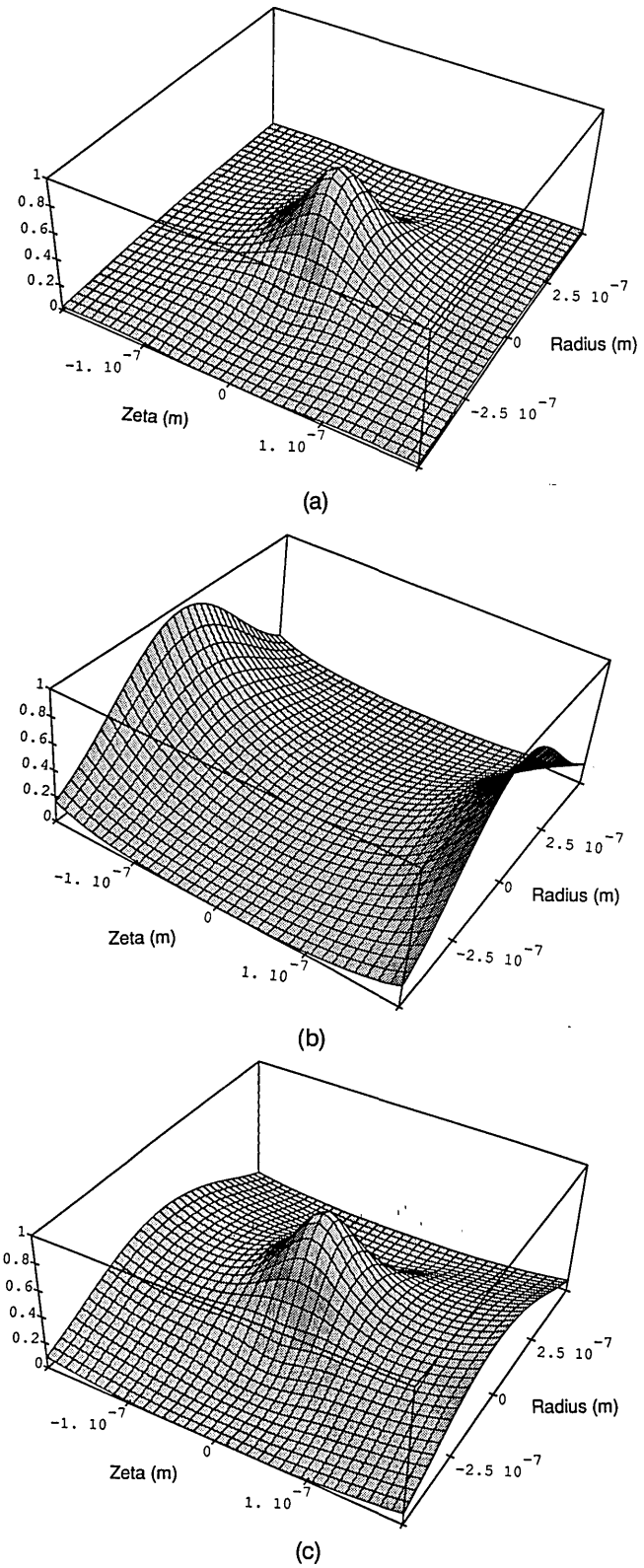

Fig. 3. MPS pulse composition for $\lambda_{max}/\lambda_{min} = 25$. (a) Normalized unperturbed free-space equivalent, $|\Psi|^2$. (b) Normalized wall term, $|\Psi_w|^2$. (c) Normalized total solution, $|\Psi_u + \Psi_w|^2$. Note that the effect of the wall term is noticeable in the final solution, in contrast to the case depicted in Fig. 2. All parameters are the same as in Fig. 2, except that $b = 8.4 \times 10^{13}$ m^{-1}.

$\rho = 0$ for $z \approx 1000$ km, the free parameter a_2 in the splash pulse spectrum should be of the order of 10^7. At the same time, we also find that, for the energy in the pulse to be maintained within the core (transverse confinement), a_2 should be in the 10^{-4}–10^{-3} range. An immediate conclusion drawn from this result is that the free parameter a_2 dictates not only the decay of the pulse but also the field confinement in the core. Hence the requirements imposed on this parameter for a well-confined, localized pulse to propagate over long distances cannot be met, as seen from the wide variance in the desired values of a_2. This example proves that the synthesis process must be carried out with caution by balancing the requirements on the different free parameters.

8. CONCLUDING REMARKS

In summary, we have shown the existence of slowly decaying, nondispersive solutions in an optical fiber waveguide. A novel bidirectional decomposition of solutions to the scalar wave equation into multiplicatively backward- and forward-traveling plane waves was applied to an optical fiber operated in the linear region. Four choices of the source spectra were considered, and closed-form solutions were obtained. The MPS pulse proved that, even though the solution deviated from the ideal MPS pulse owing to the waveguiding constraint, a proper choice of the free parameters could lead to large distances over which the pulse would maintain its original amplitude. We also showed that the synthesis process leading to exact solutions needs to be performed with caution and demonstrated this in the case of the splash pulse spectrum without the delta function when it was not possible to tweak the free parameters to obtain nondecaying localized pulses confined to the fiber core. This example underscores the fact that all the spectra that have given rise to LW solutions in free space need not be suitable for generating nondispersive solutions in waveguides.

In the practical realization of localized pulse-launching schemes, the source spectra that are most easily implementable should be considered. It is not clear whether the four spectra considered in this paper will prove to be the right candidates. However, a rich class of other related spectra $A(\alpha, \beta, \kappa)$ of the form $\delta(\beta - \beta')\exp(-\alpha a_1) I_0(a_2\kappa)$, $\delta(\beta - \beta')\exp(-\alpha a_1)J_0(a_2\kappa)$, $\delta(\beta - \beta')\exp(-\alpha a_1) J_0(a_2\kappa^2/4)$, or $\alpha \exp(-\alpha a_1)\exp(-\beta a_2)\exp(-a_3/\alpha)$, which are theoretically more cumbersome, may lend themselves to easier implementation because of the extra free parameters available for tweaking. Such spectra may also reduce the restriction on the highly broadband nature of the MPS pulse spectrum described in this paper. Utilizing the full potential of the bidirectional superposition may thus pave the way for future experimental systems.

In practical fiber-optic systems, pulse dispersion is significantly affected by material properties, especially when a broadband spectrum is used as the source. To aid our analysis when material dispersion is present, we have looked at a much simpler system, namely, a plasma-filled cylindrical metallic waveguide. Our results indicate that, despite the presence of material dispersion, the localized propagation of pulses is feasible; these results will be presented elsewhere. Future theoretical efforts will include a more detailed analysis that incorporates material dispersion and losses in the fiber. Several numerical methods or asymptotic techniques available in the literature can be used to perform this analysis.[16] Despite the centrally localized nature of these solutions, the possibility of generating higher-order modes in the fiber cannot be ignored. Higher-order modes will act as noise in the system, and their effect on the localization of the fundamental solution needs to be analyzed. In the practical arena the availability of the optical equivalents of the arrays used for generating the acoustic LW's will finally determine the realizability of such schemes.

APPENDIX A: EFFECTIVE INDEX CALCULATION

A method to calculate the effective refractive index, n_e, of the cladding for a unity core refractive index is now given. The analysis is carried out in the classical notation. The underlying principle is that the expressions for the fields in the core and the cladding, as well as the eigenvalue equation, should remain unchanged by this transformation.

We first define the parameters U, W, and V as follows:

$$U = k_0 a(n_1^2 - \overline{\beta}^2)^{1/2}, \tag{A1}$$

$$W = k_0 a(\overline{\beta}^2 - n_1^2)^{1/2}, \tag{A2}$$

$$V = (U^2 + W^2)^{1/2}. \tag{A3}$$

Here $\overline{\beta} = \beta/k_0$ is the normalized propagation constant, $k_0 = 2\pi/\lambda$ is the free-space propagation constant, and a is the fiber core radius. The fields in the core and the cladding can be described completely in terms of U and W. Eigenvalue equation (18) can be expressed in the form $f(U,W) = 0$. This implies that, if by a simple transformation we can express U and W in terms of $n_1 = 1$ and $n_2 = n_e$, we will have an equivalent waveguide.

Consider the transformation, $k_0' = k_0 n_1$. We can write the transformed normalized propagation constant β' as $\beta' = \beta/k_0' = \beta/k_0 n_1$. U and W can then be expressed as

$$U = k_0' a(1 - \overline{\beta}'^2)^{1/2}, \tag{A4}$$

$$W = k_0' a\left[\overline{\beta}'^2 - \left(\frac{n_2}{n_1}\right)^2\right]^{1/2}. \tag{A5}$$

For $n_1 = 1$ and $n_e = n_2/n_1$, we now have an equivalent waveguide in a frequency-scaled system that maintains the eigenvalue equation of the fiber as well as the expressions for the fields in the core and the cladding regions.

APPENDIX B: DETAILS OF LOCALIZED-WAVE PULSE DERIVATIONS

1. Focus Wave Modelike Solution

After integrating over κ_1 and using the sifting property of the delta function, we find Ψ_u to be

$$\Psi_u(\rho,\zeta,\eta) = a_1 \int_0^\infty d\alpha J_0[(4\alpha\beta')^{1/2}\rho]\exp(-i\alpha\zeta - \alpha a_1) \times \exp(+i\beta'\eta), \tag{B1}$$

and Ψ_w is expressed as

$$\Psi_w(\rho,\zeta,\eta) = -a_1\int_0^{\alpha'} d\alpha J_0[(4\alpha\beta')^{1/2}\rho]\exp(-i\alpha\zeta - \alpha a_1) \times \exp(+i\beta'\eta), \quad \text{(B2)}$$

where $\alpha' = \beta$'s.

We first obtain a closed-form solution for Ψ_u. Using identity (6.614.1) from Gradshteyn and Ryzhik,[17] viz.,

$$\int_0^\infty d\beta J_0(\sqrt{\beta}b)\exp(-\beta a) = \frac{b}{4}\left(\frac{\pi}{a^3}\right)^{1/2}\exp\left(-\frac{b^2}{8a}\right) \times \left[I_{-1/2}\left(\frac{b^2}{8a}\right) - I_{1/2}\left(\frac{b^2}{8a}\right)\right], \quad \text{(B3)}$$

and the Bessel-function relation

$$[I_{-1/2}(z) - I_{1/2}(z)] = \left(\frac{2}{\pi z}\right)^{1/2}\exp(-z), \quad \text{(B4)}$$

we obtain the relation

$$\int_0^\infty d\beta J_0(b\sqrt{\beta})\exp(-\beta a) = \frac{1}{a}\exp\left(-\frac{b^2}{4a}\right). \quad \text{(B5)}$$

From Eqs. (B1) and (B5) we then obtain the FWM solution

$$\Psi_u(\rho,\zeta,\eta) = a_1\frac{\exp(i\beta'\eta)}{(a_1 + i\zeta)}\exp\left[-\frac{\beta'\rho^2}{(a_1 + i\zeta)}\right]. \quad \text{(B6)}$$

We can rewrite the expression for Ψ_w, Eq. (B2), as

$$\Psi_w(\rho,\zeta,\eta) = -2a_1\exp(+i\beta'\eta)\int_0^{\sqrt{\alpha'}} w dw J_0[(4\beta')^{1/2}\rho w] \times \exp[-w^2(a_1 + i\zeta)], \quad \text{(B7)}$$

where we have made the substitution $w^2 = \alpha$. Using identity (1.8.2.4) from Prudnikov *et al.*,[18] namely,

$$\int_0^x x^{\nu+1}\exp(ax^2)J_\nu(bx)dx = \frac{b^\nu\exp(ax^2)}{(2ia)^{\nu+1}} \times [U_{\nu+1}(2iax^2, bx) + iU_{\nu+2}(2iax^2, bx)], \quad \text{(B8)}$$

where

$$U_n(z,\zeta) = \sum_{k=0}^{\infty}(-1)^k\left(\frac{z}{\zeta}\right)^{2k+\nu}J_{2k+\nu}(\zeta) \quad \text{(B9)}$$

is the Lommel function of two variables, we obtain

$$\Psi_w = \frac{ia_1}{(a_1 + i\zeta)}\exp[-\beta'(a_1 + i\zeta)s] \times \{U_1[-2i\beta'(a_1 + i\zeta)s, 2\rho\beta'\sqrt{s}] + iU_2[-2i\beta'(a_1 + i\zeta)s, 2\rho\beta'\sqrt{s}]\}, \quad \text{(B10)}$$

which gives us the final closed-form solution for the wall term.

2. Splash Pulse

Substituting the splash pulse spectrum [Eq. (34)] into the expression for the generalized solution of the scalar wave equation [Eq. (20)] and integrating over β and κ_1, we get

$$\Psi(\rho,\zeta,\eta) = 2\gamma a_1 a_2 J_0(\gamma\rho)\int_{\gamma\sqrt{s}/2}^\infty \frac{d\alpha}{4\alpha}\exp[-\alpha(a_1 + i\zeta)] \times \exp\left[-\frac{\gamma^2}{4\alpha}(a_2 - i\eta)\right]. \quad \text{(B11)}$$

Breaking the solution into Ψ_u and Ψ_w and using identity (2.3.16.1) from Prudnikov *et al.*,[18] namely,

$$\int_0^\infty \frac{dx}{x}\exp(-xa)\exp\left(-\frac{b}{x}\right) = 2K_0[2(ab)^{1/2}], \quad \text{(B12)}$$

we can arrive at the expressions

$$\Psi_u = a_1 a_2 \gamma J_0(\gamma\rho)K_0\{\gamma[(a_1 + i\zeta)(a_2 - i\eta)]^{1/2}\}, \quad \text{(B13)}$$

$$\Psi_w = -\frac{a_1 a_2 \gamma}{2}\int_0^{\gamma\sqrt{s}/2}\frac{d\alpha}{\alpha}\exp[-\alpha(a_1 + i\zeta)] \times \exp\left[-\frac{\gamma^2}{4\alpha}(a_2 - i\eta)\right]. \quad \text{(B14)}$$

3. Hillion's Splash Modes

a. Integrate over β First

Substituting the Bessel spectrum [Eq. (37)] into expression (28) and integrating over κ_1, we obtain

$$\Psi(\rho,\zeta,\eta) = a_1 b\int_0^\infty d\alpha\exp[-\alpha(a_1 + i\zeta)] \times \int_0^{\alpha'} d\beta J_0[(4\alpha\beta)^{1/2}\rho]J_0(\beta b)\exp(i\beta\eta), \quad \text{(B15)}$$

where $\alpha' = \alpha/s$. When we substitute $\beta = r\cos\theta$, $\alpha = r\sin\theta$, and $d\alpha d\beta = rdrd\theta$, Eq. (B15) becomes

$$\Psi(\rho,\zeta,\eta) = a_1 b\int_0^{\theta'} d\theta\int_0^\infty r dr J_0[(4\sin\theta\cos\theta)^{1/2}\rho r] \times J_0(br\sin\theta) \times \exp\{-r[\cos\theta(a_1 + i\xi) - i\eta\sin\theta]\}, \quad \text{(B16)}$$

where $\tan\theta' = 1/s$. Using identity (2.12.38.2) from Prudnikov *et al.*,[18] namely,

$$\int_0^\infty dx x J_0(bx)J_0(cx)\exp(-px) = A_{0,0}{}^2, \quad \text{(B17)}$$

where

$$A_{0,0}{}^2 = \frac{-\rho k^2(qd)^{-3/2}}{2\pi(1 - k^2)^{1/2}}Q_{-1/2}{}^1\left(\frac{2 - k^2}{k^2}\right), \quad \text{(B18)}$$

we obtain

$$\Psi = a_1 b\int_0^{\theta_1} d\theta\frac{p}{(qd)^{1/2}[(p^2 + q^2 + d^2) - 4q^2d^2]^{1/2}}Q_{-1/2}{}^1 \times \left(\frac{p^2 + q^2 + d^2}{2qd}\right). \quad \text{(B19)}$$

Here $k^2 = 4qc/[p^2 + (b + d)^2]$, $p = (a_1 + i\zeta)\cos\theta - i\eta\sin\theta$, $q = 2\rho(\sin\theta\cos\theta)^{1/2}$, and $d = b\sin\theta$. $Q_n{}^m(z)$, an associated Legendre function, is a solution of the dif-

ferential equation

$$(1 - z^2)\frac{d^2Q_n^m}{dz^2} - 2z\frac{dQ_n^m}{dz} + \left[n(n+1) - \frac{m^2}{1-z^2}\right]Q_n^m = 0. \tag{B20}$$

b. Integrate over α First

Substituting the Bessel spectrum [Eq. (37)] into expression (29), integrating over κ_1, and breaking the solution into two parts, Ψ_u and Ψ_w, we obtain

$$\Psi_u(\rho,\zeta,\eta) = ba_1\int_0^\infty d\beta\int_0^\infty d\alpha\,\exp[-\alpha(a_1 + i\zeta)] \times J_0[(4\alpha\beta)^{1/2}\rho]J_0(\beta b)\exp(i\beta\eta). \tag{B21}$$

Using identities (2.12.39.10) and (2.12.8.3) from Prudnikov *et al.*,[18] namely,

$$\int_0^\infty \exp(-ipx)J_0(c\sqrt{x})J_0(bx)dx = \frac{1}{(b^2 - p^2)^{1/2}} \times \exp\left[-\frac{ic^2p}{4(b^2-p^2)}\right]J_0\left[\frac{c^2b}{4(b^2-p^2)}\right], \tag{B22}$$

$$\int_0^\infty \exp(-ipx)J_0(cx)dx = \frac{1}{(c^2 - p^2)^{1/2}}, \tag{B23}$$

respectively, we obtain the following expression for the unperturbed pulse:

$$\Psi_u = \frac{ba_1}{(a_1 + i\zeta)}\left\{\left[\frac{\rho^2}{(a_1+i\zeta)} - i\eta\right]^2 + b^2\right\}^{-1/2}. \tag{B24}$$

The contribution from the wall term, Ψ_w, can be written as

$$\Psi_w(\rho,\zeta,\eta) = -a_1b\int_0^\infty d\beta J_0(\beta b)\exp(i\beta\eta) \times \int_0^{\beta s} d\alpha\,\exp[-\alpha(a_1 + i\zeta)]J_0[(4\alpha\beta)^{1/2}\rho]. \tag{B25}$$

The integral over α is of the same form as Eq. (B2). Using an approach similar to that adopted for solving Eq. (B2), we obtain

$$\Psi_w = \frac{ia_1b}{(a_1+i\zeta)}\int_0^\infty d\beta\,\exp\{-\beta[(a_1 + i\zeta)s - i\eta]\} \times \{U_1[-2i\beta(a_1+i\zeta)s, 2\rho\beta\sqrt{s}\,] + iU_2[-2i\beta(a_1+i\zeta)s, 2\rho\beta\sqrt{s}\,]\}. \tag{B26}$$

4. Modified Power Spectrum

We substitute the MPS pulse spectrum [Eq. (41)] into expression (29) and separate the integral into two parts, viz.,

$$\Psi = \Psi_u + \Psi_w = \int_0^\infty d\kappa_1\int_0^\infty d\alpha\int_0^{\alpha/s} d\beta I - \int_0^\infty d\kappa_1\int_0^\infty d\alpha\int_{\alpha/s}^\infty d\beta I, \tag{B27}$$

where Ψ_u and Ψ_w correspond to the first and the second terms, respectively. We first evaluate Ψ_u. Integrating over α first, we can write Ψ_u as

$$\Psi_u = \frac{p}{8\pi}\int_{b/p}^\infty \frac{d\beta}{\beta}\exp[(-\beta p + b)a_2 + i\eta] \times \int_0^\infty d\kappa_1\kappa_1 J_0(\kappa_1\rho)\exp\left[-\frac{\kappa_1^2(a_1+i\zeta)}{4\beta}\right]. \tag{B28}$$

Using the identity equation (B5) and integrating over κ_1 and β, we obtain

$$\Psi_u(\rho,\zeta,\eta) = \frac{\exp[-(b\chi/p)]}{4\pi(a_1+i\zeta)(a_2+\chi/p)}, \tag{B29}$$

which is identical to the MPS pulse derived by Besieris *et al.*[6]

To evaluate Ψ_w we switch the order of integration of α and β and use the identity equation (B8) to obtain

$$\Psi_w = \frac{ip\exp(ba_2)}{2\pi(a_1+i\zeta)}\int_{b/p}^\infty d\beta\,\exp(-\beta\Omega) \times \{U_1[2i\beta(a_1+i\zeta)s, 2\rho\beta\sqrt{s}\,] + iU_2[2i\beta(a_1+i\zeta)s, 2\rho\beta\sqrt{s}\,]\}, \tag{B30}$$

where $\Omega = (pa_2 - i\eta) + s(a_1 + i\zeta)$. By expressing the Lommel functions U_1 and U_2 in terms of a series of Bessel functions [see Eq. (B9)] and switching the summation and the integral evaluation, one can show that the integrand is bounded and that an end-point evaluation of the form

$$\int_a^\infty \exp[-\beta f(x)]g(x)dx \approx \frac{\exp[-\beta f(a)]g(a)}{\beta[(df/dx)(a)]} + O(\beta^{-2}) \tag{B31}$$

is justified. Using the result from such an end-point evaluation, we arrive at the final expression for Ψ_w, viz.,

$$\Psi_w \approx \frac{ip\exp(ba_2)}{2\pi(a_1+i\zeta)}\exp\left(-\frac{b}{p}\Omega\right) \times \left\{U_1\left[2i\frac{b}{p}(a_1+i\zeta)s, 2\rho\frac{b}{p}\sqrt{s}\right] + iU_2\left[2i\frac{b}{p}(a_1+i\zeta)s, 2\rho\frac{b}{p}\sqrt{s}\right]\right\}. \tag{B32}$$

APPENDIX C: EVALUATION OF NONDECAYING PULSE DISTANCES

1. Focus Wave Mode Solution

The initial pulse amplitude of the ideal FWM solution is given by

$$|\Psi_u{}^0| = \exp\left(-\frac{\beta'\rho^2}{a_1}\right). \tag{C1}$$

The variation of the field amplitude in the radial direction is dictated by the magnitude of the ratio β'/a_1. A pulse propagating in the positive z direction has a pulse peak given by

$$|\Psi_u{}^+| = \exp\left(-\frac{\beta'\rho^2}{a_1}\right), \tag{C2}$$

which is identical to the initial pulse amplitude. The distance over which this pulse can be utilized for communications purposes depends on the losses and the material dispersion of the waveguide. Transmission of energy in the positive direction seems possible with little constraint on the free parameters of the source spectra. The wall term can be expected to impose further constraints on the pulse parameters.

2. Splash Pulse Solution

The amplitude of the unperturbed splash pulse solution, Ψ_u, evaluated at $z = t = 0$ can be expressed as

$$\Psi_u = a_1 a_2 \gamma J_0(\gamma\rho) K_0[\gamma(a_1 a_2)^{1/2}]. \tag{C3}$$

The radial dependence of the field is governed by the magnitude of γ. We need to ensure during synthesis that we do not impose any further constraints on the free parameter γ when considering the distances over which this pulse can remain nondecaying. At $z = t = 0$, $|\Psi_u{}^0|$ is given at the center of the fiber ($\rho = 0$) by the equation

$$|\Psi_u{}^0|^4 = a_1{}^3 a_2{}^3 \gamma^2 \frac{\pi^2}{4} \exp[-4\gamma(a_1 a_2)^{1/2}], \tag{C4}$$

where we have used the large-argument expansion of the Bessel function and the fourth power of the amplitude is taken only for convenience in deriving the results that follow. At $z = ct$, the amplitude of the pulse traveling in the positive direction, $|\Psi_u{}^+|$, can be written as

$$|\Psi_u{}^+|^4 = a_1{}^3 a_2{}^4 \gamma^2 \frac{\pi^2}{4(a_2{}^2 + 4z^2)^{1/2}} \times \exp[-4\gamma\sqrt{a_1}(a_2{}^2 + 4z^2)^{1/4} \cos\phi], \tag{C5}$$

where ϕ is given by the relation $\tan 2\phi = 2z/a_2$. Expressing $\cos\phi$ in terms of z and a_2, using the approximation $a_2 \gg z$ of interest, and defining a decay factor Γ^4 as $|\Psi_u{}^+|^4/|\Psi_u{}^0|^4$, we obtain an estimate for the nondecaying pulse distances. The decay factor Γ^4 can be written as

$$\Gamma^4 = \left(1 + \frac{4z^2}{a_2{}^2}\right)^{-1/2} \exp\left[-2\gamma(a_1 a_2)^{1/2} \frac{z^2}{a_2{}^2}\right], \tag{C6}$$

which shows that, for the decay factor to remain ≈ 1, the value of the free parameter a_2 should be a few orders of magnitude greater than the distance, z, of interest. Note also that the nondecaying nature of the solution does not depend on the value of γ, which defined the confinement of the field in the fiber core.

3. Scalar Analog to Hillion's Spinor Modes

The amplitude of the unperturbed pulse expression for the Bessel spectrum can be written, at $z = t = 0$, as

$$\Psi_u = \left[1 + \left(\frac{\rho^2}{a_1 b}\right)^2\right]^{-1/2}. \tag{C7}$$

The corresponding expressions for $|\Psi_u{}^0|$ and $|\Psi_u{}^+|$ are

$$|\Psi_u{}^0| = 1, \tag{C8}$$

$$|\Psi_u{}^+| = \left(1 - \frac{4z^2}{b^2}\right)^{-1/2}. \tag{C9}$$

The decay factor Γ has the same expression as $|\Psi_u{}^+|$, given by Eq. (C9), and we note that the pulse in the positive direction is singular at $\rho = 0$ and $z = b/2$. This behavior of the unperturbed, ideal pulse is physically unrealizable. If the wall term Ψ_w cancels this singularity, the sensitivity to variations in initial distribution may make this pulse extremely difficult to realize in a practical sense.

4. Splash Pulse Spectrum without the Delta Function

In all the previous examples in this appendix we considered the effect of the free parameters on the ideal pulse shapes. The only total pulse ($\Psi_u + \Psi_w$) that we considered was the MPS pulse in the main text of this paper. We now investigate the case in which the free parameters cannot be tweaked to generate a pulse that will propagate for long distances and at the same time be confined to the fiber core. Consider the splash pulse spectrum without the delta function $\delta(\kappa - \gamma)$. After going through lengthy algebra we can show that the final expression for this pulse is given by

$$\Psi = \frac{a_1 a_2}{(a_1 + i\zeta)} \{4\rho^2 s + [(a_1 + i\zeta)s + (a_2 - i\eta)]^2\}^{-1/2}. \tag{C10}$$

The initial pulse amplitude is given by

$$|\Psi^0| = a_2[4\rho^2 s + (a_1 s + a_2)^2]^{-1/2}. \tag{C11}$$

At the center of the fiber core, the amplitude of the pulse traveling in the positive direction can be written as

$$|\Psi^+| = a_2[4z^2 s + (a_1 s + a_2)^2]^{-1/2}. \tag{C12}$$

As a result, the decay factor, Γ, can be expressed in the form

$$\Gamma = \frac{|\Psi^+|}{|\Psi^0|} = \left[1 + \frac{4z^2 s}{(a_1 s + a_2)^2}\right]^{-1/2}. \tag{C13}$$

From Eq. (C11), the variation of the initial field amplitude in the core can be plotted versus the radius ρ as shown in Fig. 4. The variation of the decay factor, Γ, is given in Fig. 5, where we have made the assumption that $a_1 s \ll a_2$. Figure 4 shows that, to confine the field to the core, the free parameter values should be of the order of 10^{-4}–10^{-5}. At the same time, Fig. 5 shows that the decay factor

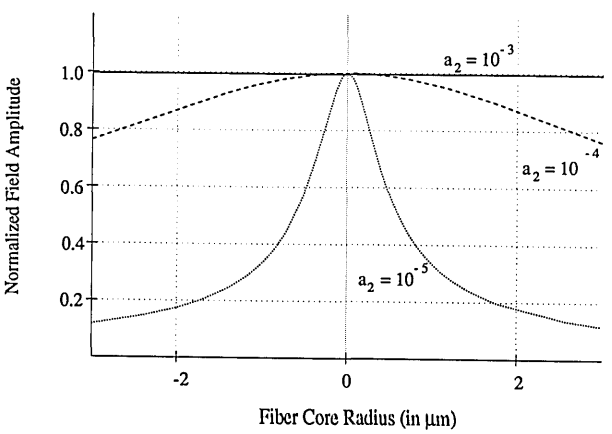

Fig. 4. Dependence of the field confinement in the fiber on the free parameter a_2 for the splash pulse. For guided confinement of the field power, a_2 values of the order of 10^{-5} will be preferred.

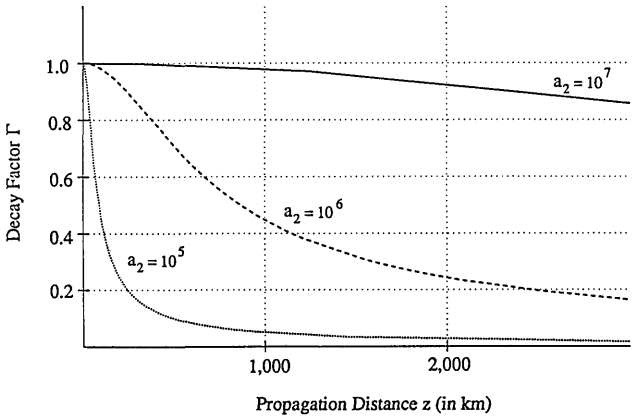

Fig. 5. Variation of the decay factor Γ as a function of the free parameter a_2 for the splash pulse. Note that for nondecaying transmission of energy the values of a_2 should be of the order of 10^7, which contradicts the requirement imposed on the field confinement as seen from Fig. 4.

will remain close to 1 for a_2 values of the order of 10^7 if nondecaying solutions over 1000-km distances are desired. This shows that the free parameter a_2 dictates both the variation of the field within the core and the distance over which the field remains nondecaying and that it cannot meet the requirements.

ACKNOWLEDGMENTS

This research was supported in part by the Lawrence Livermore Laboratory and the Virginia Center for Innovative Technology.

*Present address, AT&T Bell Laboratories, Murray Hill, New Jersey 07974-0636.

REFERENCES AND NOTES

1. J. N. Brittingham, "Focus wave modes in homogeneous Maxwell's equations: transverse electric mode," J. Appl. Phys. **54,** 1179–1189 (1983).
2. R. W. Ziolkowski, "Localized transmission of electromagnetic energy," Phys. Rev. A **39,** 2005–2033 (1989).
3. R. W. Ziolkowski and D. K. Lewis, "Verification of the localized wave transmission effect," J. Appl. Phys. Rev. **68,** 6083–6085 (1990).
4. J. Durnin, "Exact solutions for nondiffracting beams. I. The scalar theory," J. Opt. Soc. Am. A **4,** 651–654 (1987).
5. J. Durnin, J. J. Miceli, and J. H. Eberly, "Diffraction free beams," Phys. Rev. Lett. **58,** 1499–1501 (1987).
6. I. M. Besieris, A. M. Shaarawi, and R. W. Ziolkowski, "A bidirectional travelling plane wave representation of exact solutions of the scalar wave equation," J. Math. Phys. **30,** 1254–1269 (1989).
7. P. Hillion, "Spinor focus modes," J. Math. Phys. **28,** 1743–1748 (1987).
8. A. M. Shaarawi, I. M. Besieris, and R. W. Ziolkowski, "Localized energy pulse trains launched from an open, seni-infinite, circular waveguide," J. Appl. Phys. **65,** 805–813 (1989).
9. R. W. Ziolkowski, I. M. Besieris, and A. M. Shaarawi, "Aperture realizations of exact solutions to homogeneous wave equations," J. Opt. Soc. Am. A (to be published).
10. A. Hasegawa and F. Tappert, "Transmission of stationary nonlinear optical pulses in dispersive dielectric fibers. I. Anomalous dispersion," Appl. Phys. Lett. **23,** 142–144 (1973).
11. L. F. Mollenauer, R. H. Stolen, and J. P. Gordon, "Experimental observation of picosecond pulse narrowing and solitons in optical fibers," Phys. Rev. Lett. **45,** 1095–1097 (1980).
12. D. Gloge, "Weakly guiding fibers," Appl. Opt. **10,** 2252–2258 (1971).
13. P. A. Belanger, "Packetlike solutions of the homogeneous-wave equation," J. Opt. Soc. Am. A **1,** 723–724 (1984).
14. A. Sezginer, "A general formulation of focus wave modes," J. Appl. Phys. **57,** 678–683 (1985).
15. R. W. Ziolkowski, "Exact solutions of the wave equation with complex source locations," J. Math. Phys. **26,** 861–863 (1985).
16. For example, see K. A. Connor and L. B. Felsen, "Complex space-time rays and their application to pulse propagation in lossy dispersive media," Proc. IEEE **62,** 1586–1598 (1974); K. E. Oughstun and G. E. Sherman, "Propagation of electromagnetic pulses in linear dispersive medium with absorption (the Lorentz medium)," J. Opt. Soc. Am. B **5,** 817–849 (1988).
17. I. S. Gradshteyn and I. M. Ryzhik, *Tables of Integrals, Series and Products* (Academic, New York, 1965).
18. A. P. Prudnikov, Y. A. Bruchkov, and O. I. Marichev, *Integrals and Series. Volume 2: Special Functions* (Gordon & Breach, New York, 1986).